

# Improvement of Mathematical Models with Time-Shift of Two- and Tri-Fragment Signals with Non-Linear Frequency Modulation

*Kostyria O. O.<sup>1</sup>, Hryzo A. A.<sup>1</sup>, Dodukh O. M.<sup>1</sup>, Nariezhnii O. P.<sup>2</sup>*

<sup>1</sup>Ivan Kozhedub Kharkiv National Air Force University, Kharkiv, Ukraine

<sup>2</sup>V. N. Karazin Kharkiv National University, Kharkiv, Ukraine

E-mail: [oleksandr.kostyria@nure.ua](mailto:oleksandr.kostyria@nure.ua)

The use of signals with intra-pulse modulation in radar systems allows us to increase the duration of sounding pulses, and therefore the radiated energy with limitations on peak power. In the processing system, compression of the signal provides the necessary time difference, but leads to the appearance of side lobes. This, in turn, causes the “stretching” of the passive interference zone by range and worsens the potential for target detection. Therefore, reducing the level of the side lobes of the processed signal is an urgent task of radar. With regard to the maximum level of side lobes, signals with non-linear frequency modulation have advantages, but the models used for their mathematical description need to be clarified. The research carried out by the authors of the article and the obtained results of mathematical modelling explain the mechanism of frequency and phase jumps in signals with nonlinear frequency modulation, consisting of several linearly frequency modulated fragments. These results are obtained for the mathematical model of the current time, when the time of each subsequent fragment is counted from the end of the previous one. The article discusses mathematical models of two- and three-fragment signals with using different approach. The difference is that the start time of each successive linearly frequency modulated fragment is shifted to the origin, that is, the shifted time is used. The advantage of this approach is the absence of frequency jumps at the joints of fragments, but phase jumps at these moments of time still occur. Thus, there is a need to develop a mathematical apparatus for compensating of such jumps. An analysis of known publications conducted in the first section of the article shows that for mathematical models of shifted time, the issue of determining the magnitude of phase jumps at the joints of fragments and the mechanisms for their compensation were not considered. From this follows the task of research, which is formulated in the second section of the work. Mathematical calculations for determining the magnitude of phase jumps that occur in these mathematical models, as well as the results of checking the improved mathematical apparatus, are given in the third section of the work. Further research is planned to be directed at the features of using the developed mathematical models in solving applied problems in radar systems.

*Keywords:* signals with nonlinear frequency modulation; mathematical model; instantaneous phase jump; autocorrelation function; maximum level of side lobes

DOI: [10.20535/RADAP.2023.93.22-30](https://doi.org/10.20535/RADAP.2023.93.22-30)

## Statement of the research task

Signals with internal pulse frequency (phase) modulation make it possible to increase the duration of the probing radio pulse while maintaining time discriminating ability. Linearly frequency modulated (LFM) signals [1–6] are widely used, their significant drawback is a rather high maximum peak of side lobes level (MPSLL, SLL) of the autocorrelation function (ACF).

In the presence of a high SLL, an excessive increase in the signal base (the product of the width of the radio pulse spectrum by its duration) leads to a “stretching” of the passive interference zone by range. Such a zone can expand by 20...30%, which is a significant share of the maximum detection range [7, 8].

One approach to reducing this effect is to decrease the MPSLL of signals at the output of processing devices by using probing signals with non-linear frequency modulation (NLFM, FM). NLFM are widely used in the form of a sequential combination of fragments with linear or nonlinear laws of FM [9–15]. The authors show the presence of jumps of instantaneous frequency and phase at the joints of fragments of the NLFM signal, which consists of two and three LFM fragments, and proposed a mechanism for their compensation for the mathematical model (MM) of the current time [16]. It is proposed to introduce the used approach to the model of shifted time of two- and three-fragment NLFM signals [9, 10, 12–14].

As a task of the study, we will determine the finding of the phase jumps at the joints of LFM fragments of NLFM signals and the development of a mechanism for their compensation in order to reduce MPSLL.

## 1 Analysis of studies and publications

In modern radars, chirp signals are often used to detect targets and accompany them, since due to the comb form of the autocorrelation function, they are weakly sensitive to Doppler frequency shift, which simplifies their [1–6]. The capabilities of LFM signals are significantly expanded if the frequency modulation rate in individual signal fragments varies according to a certain linear or non-linear law, such signals belong to the class of NLFM signals.

Change of frequency modulation rate during signal duration allows us to reduce level of side lobes on frequency-time plane [1–6]. Many publications on the subject of the work are devoted to the study of various methods for the development and optimization of LFM and NLFM signals [1–6, 16–26], the presentation of the material is carried out taking into account the requirements and limitations of specific radar applications.

The works are generally aimed at minimizing MPSLL and strive to achieve optimal time and frequency resolution, efficient use of energy of sounding signals.

The authors [27–35] consider NLFM signals as an effective means to solve a variety of applications due to a greater degree of reduction in MPSLL. Research in this area is focused on the development of synthesis algorithms and methods for processing received signals. The papers present MM of various NLFM signals [1–6, 14, 16, 19, 25, 29, 32–35], and a number of studies consider the specific applications and results of experiments [4, 10, 27, 30].

## 2 Formulation of the study task

The aim of the work is to improve mathematical models with time shift of NLFM signals, consisting of two and three LFM fragments, by determining the magnitude of phase jumps at their joints and developing a mechanism for compensating of these jumps.

## 3 Presentation of the study material

### 3.1 Improvement of mathematical model with time shift for two-fragment NLFM signal

Consider the NLFM signal, which consists of two LFM fragments [9, 12–14, 16, 20, 22, 26]. Mathematical model (MM) for the instantaneous phase of such a signal has the form:

$$\varphi_n(t) = 2\pi \begin{cases} f_0 t \pm \frac{\beta_1}{2} t^2, & 0 \leq t \leq T_1; \\ (f_0 + \beta_1 T_1)(t - T_1) \pm \frac{\beta_2}{2} (t^2 - T_1 t), & T_1 \leq t \leq T_1 + T_2, \end{cases} \quad (1)$$

where  $f_0$  – initial frequency of NLFM signal;  $\beta_1, \beta_2$  – frequency modulation rate of the first and second FM fragments:

$$\beta_1 = \frac{\Delta f_1}{T_1}; \quad \beta_2 = \frac{\Delta f_2}{T_2},$$

where  $\Delta f_1, \Delta f_2$  – frequency deviation (difference between upper and lower frequencies) of the corresponding FM fragment;  $T_1, T_2$  – duration of the first and second signal fragments.

The sign «+» or «-» in (1) means that the instantaneous phase of the NLFM signal increases or decreases in time, so we have a linear increase or decrease in the frequency of fragments. Expressions for instantaneous frequencies of fragments of the NLFM signal are obtained from (1) by differentiation, one of the options for plotting the frequency versus time is shown in Fig. 1 (solid line). This case demonstrates a decrease in frequency with increasing time.

From analysis (1) and Fig. 1, it can be seen that the calculation of the parameters of the LFM fragment of the signal at the moment of time  $t = T_1$  begins with a zero count of time, that is  $t = (t - T_1) = 0$ . In fact, the graph of the change in the instantaneous frequency of the second fragment (Fig. 1, dashed line) shifts in time by an amount  $T_1$  (shown by arrows).

From (1), it is obtained that there is no frequency jump at times  $t = T_1$  because the instantaneous value of the finite frequency of the first fragment is equal to the initial value of the instantaneous frequency of the second fragment. This indicates the insensitivity of this MM to frequency jumps that occur for the MM NLFM signal in the current time [11, 15, 16], which is an advantage of such an MM NLFM signal.

Let us consider in detail how the instantaneous phase (1) changes at the moment of transition from the first fragment to the second. Consider the case of reducing the instantaneous phase (frequency) of the signal.

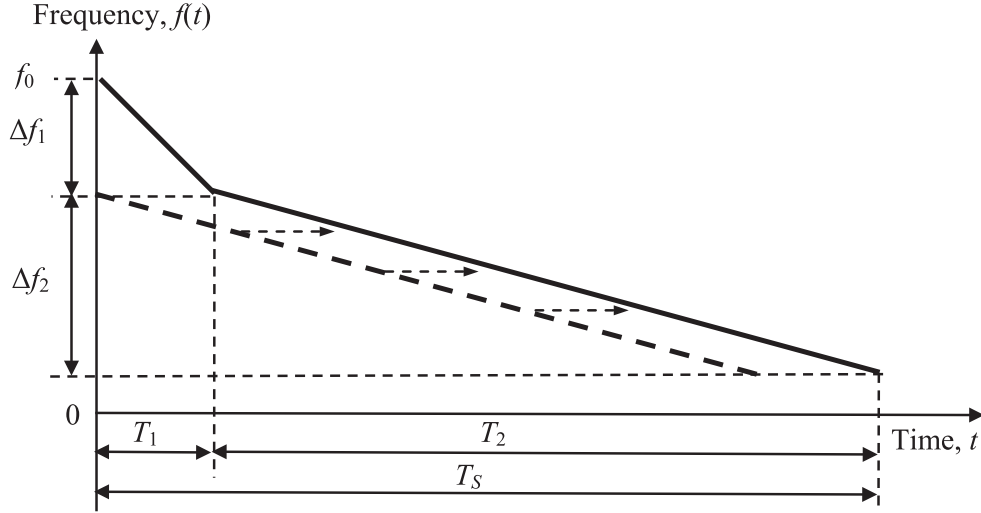


Fig. 1. Diagram of frequency variation of NLFM signal consisting of two LFM fragments

Final phase of the first LFM fragment:

$$\varphi_{E1} = 2\pi \left( f_0 T_1 - \beta_1 \frac{T_1^2}{2} \right),$$

the initial phase of the second fragment:

$$\begin{aligned} \varphi_{02} &= 2\pi \left[ f_0 t - \beta_2 \left( \frac{t^2}{2} - T_1 t \right) \Big|_{t=T_1} \right] = \\ &= 2\pi \left( f_0 T_1 + \frac{1}{2} \beta_2 T_1^2 \right). \end{aligned}$$

Find the phase jump  $\delta\varphi_{12}$  value at the moment of transition to the second fragment:

$$\delta\varphi_{12} = \varphi_{02} - \varphi_{E1} = \pi T_1^2 (\beta_2 + \beta_1). \quad (2)$$

That is, when MM (1) is used, at the moment of transition from the first LFM fragment to the second, a phase jump occurs, the magnitude of which is determined in accordance with (2).

It is proposed to improve the known MM (1) by introducing a compensating phase component (2) to compensate for this jump.

The improved MM of the two-fragment NLFM signal has the following form:

$$\varphi(t) = 2\pi \begin{cases} f_0 t - \frac{\beta_1 t^2}{2}, & 0 \leq t \leq T_1; \\ (f_0 - \Delta f_1)(t - T_1) - \beta_2 \left( \frac{t^2}{2} - T_1 t \right) - \delta\varphi_{12}, & T_1 \leq t \leq T_1 + T_2. \end{cases} \quad (3)$$

It should be noted that despite the similarity of the approach and the identity of the physical content of the components that are taken into account, the magnitude of the compensating phase component in model (3)

differs from that in the current time model [16]. The considered example is illustrative in nature and is not provided to explain the approach used. Next, consider the case of a three-fragment NLFM signal, which is widely used in solving applied problems.

### 3.2 Improvement of mathematical model with time shift for three-fragment NLFM signal

Consider the three-fragment NLFM signal [10, 14, 20, 22], the graph of the instantaneous frequency change of which is shown in Fig. 2 (solid line).

The MM of the instantaneous phase of the three-fragmented NLFM signal, the instantaneous frequency of which varies in accordance with Fig. 2, is described by expression (4) [10, 14, 20, 22]:

$$\varphi_n(t) = 2\pi \begin{cases} f_0 t - \frac{\beta_1 t^2}{2}, & 0 \leq t \leq T_1; \\ (f_0 - \Delta f_1)(t - T_1) - \beta_2 \left( \frac{t^2}{2} - T_1 t \right), & T_1 \leq t \leq T_{12}; \\ (f_0 - \Delta f_{12})(t - T_{12}) - \beta_3 \left( \frac{t^2}{2} - T_{12} t \right), & T_{12} \leq t \leq T_s, \end{cases} \quad (4)$$

where  $\Delta f_{12} = \Delta f_1 + \Delta f_2$ ;  $T_{12} = T_1 + T_2$ ;  $T_s = T_1 + T_2 + T_3$ ;  $\beta_3$  - frequency modulation rate of the third FM fragment:

$$\beta_3 = \frac{\Delta f_3}{T_3},$$

$\Delta f_3$  - frequency deviation of the third chirp fragment;  $T_3$  - duration of the third signal fragment.

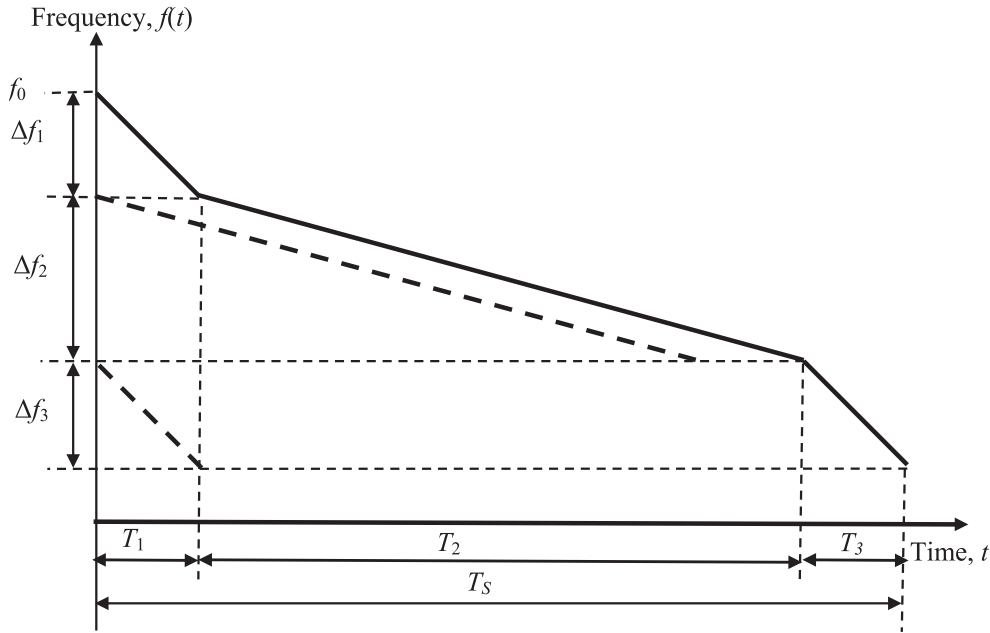


Fig. 2. Graph of frequency change of three-fragment NLFM signal

Using an approach similar to that described in subsection 3.1, we find a jump in the instantaneous phase of the NLFM signal at the junction of the second and third LFM fragments:

$$\delta\varphi_{23} = \varphi_{03} - \varphi_{E2} = \pi [T_1^2(\beta_3 + \beta_1) + T_2^2(\beta_3 + \beta_2)]. \quad (5)$$

For a three-fragment NLFM signal, taking into account (2) and (5), we obtain an improved MM with compensation for phase jumps at the moments of transition from the previous to the next LFM fragments:

$$\varphi_n(t) = 2\pi \begin{cases} f_0 t - \frac{\beta_1}{2} t^2, & 0 \leq t \leq T_1; \\ (f_0 - \Delta f_1)(t - T_1) - \beta_2 \left( \frac{t^2}{2} - T_1 t \right) - \delta\varphi_{12}, & T_1 \leq t \leq T_{12}; \\ (f_0 - \Delta f_{12})(t - T_{12}) - \beta_3 \left( \frac{t^2}{2} - T_{12} t \right) - \delta\varphi_{23}, & T_{12} \leq t \leq T_s. \end{cases} \quad (6)$$

Verification of the obtained theoretical results is carried out by comparative analysis of oscillograms, spectra and ACF, built using the known and proposed MM two-fragment (1), (3) and three-fragment (4), (6) NLFM signals.

### 3.3 Results of mathematical modelling

Verification of the validity and adequacy of improved MM was carried out in the MATLAB application package.

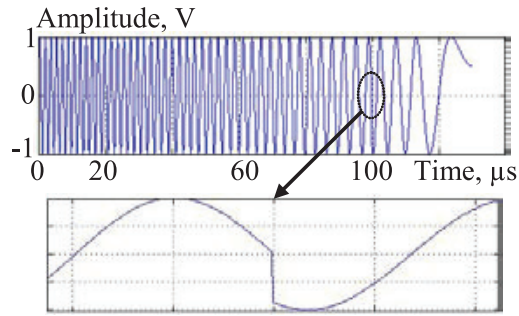
For a two-fragment NLFM signal, modelling was carried out using the following parameters: deviations of the frequency of LFM fragments are  $\Delta f_1 = 350$  kHz,  $\Delta f_2 = 250$  kHz, their duration  $T_1 = 100$   $\mu$ s,  $T_2 = 30$   $\mu$ s, respectively.

Results of modelling by ratios (1) are shown in Fig. 3 and by ratios (3) – in Fig. 4. For better visualization of the results during modelling, it is accepted  $f_0 = \Delta f_1 + \Delta f_2$ .

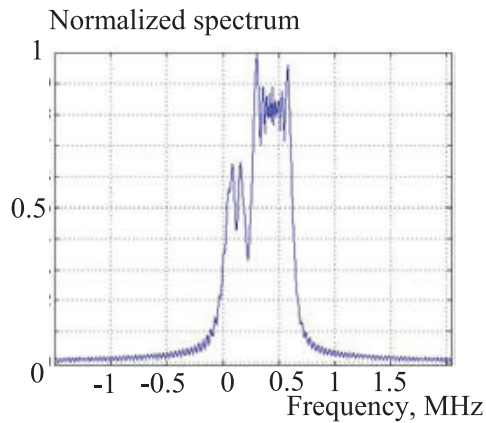
The oscillogram of the NLFM signal in Fig. 3a shows a phase jump at 100  $\mu$ s (detailed on an enlarged scale), which corresponds to the junction of fragments. The presence of a phase jump is manifested in the signal spectrum of Fig. 3b in the form of a dip at a frequency of 250 kHz, pulsation distortions of slopes, a bevelled top of the spectrum.

Due to the modification of the spectrum shape (Fig. 3b), in comparison with the classic LFM signal, the MPLSS level decreased to -14.41 dB (Fig. 3c), while the width of the GP at the zero level is 6.34  $\mu$ s. The level of the side lobes of the ACF has symmetric differences of the “step” type relative to zero, the length of which is determined by the duration of the first LFM fragment.

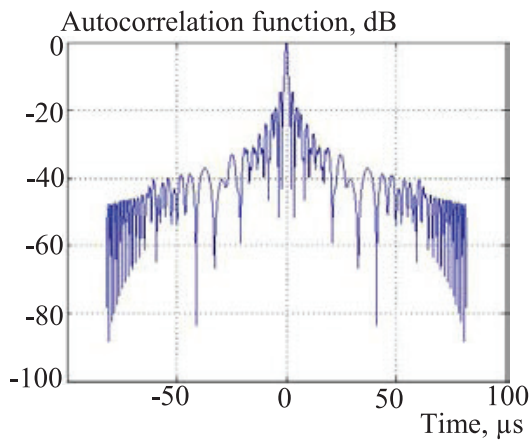
The oscillogram of the NLFM signal according to the improved model (3) is shown in Fig. 4a. Unlike model (1), the instantaneous phase of the signal changes smoothly, the phase jump is compensated (the joint of the fragments at 100  $\mu$ s is detailed). The signal spectrum is shown in Fig. 4b, there are no additional distortions, which is consistent with the theory.



(a)



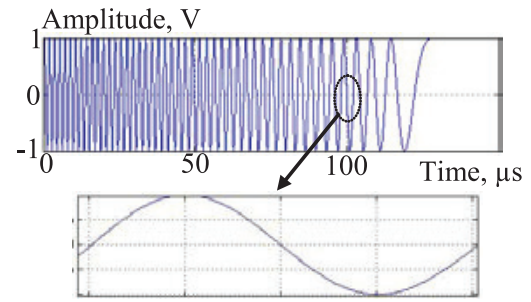
(b)



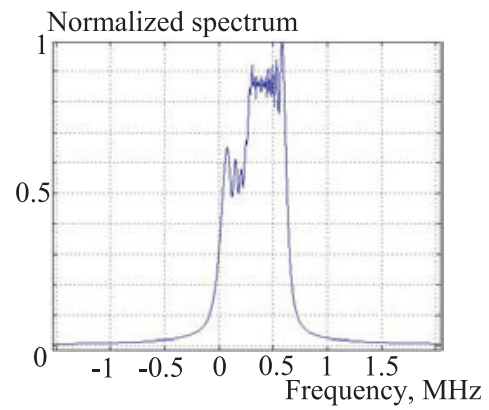
(c)

Fig. 3. Oscilloscope with detail at the junction of the fragments (a), spectrum (b), ACF (c) according to model (1)

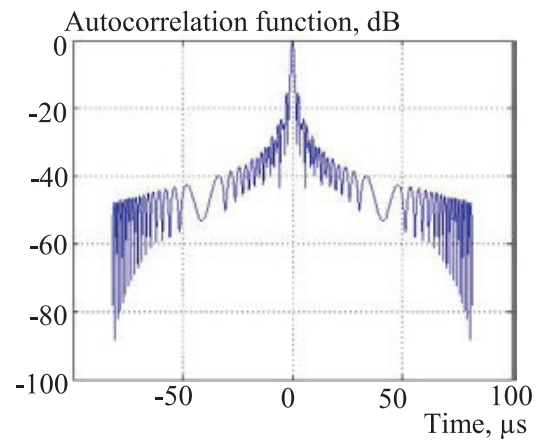
The corresponding ACF is shown in Fig. 4c, it has an MPLSS of -15.81 dB and a main lobe (ML) width at a zero level of 6.44  $\mu\text{s}$ , the level and frequency of side pulsations changes smoothly, which is also a sign of the absence of distortion of the instantaneous phase of the NLFM signal.



(a)



(b)

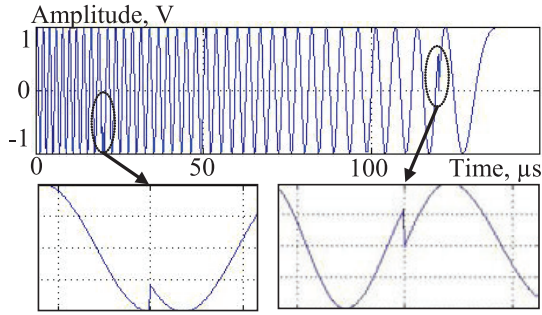


(c)

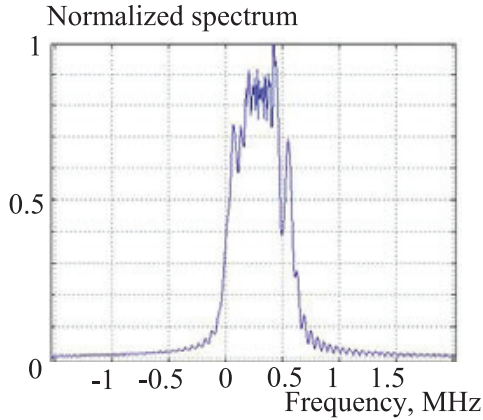
Fig. 4. Oscilloscope with detail at the junction of the fragments (a), spectrum (b), ACF (c) according to model (3)

The simulation results for the three-fragment NLFM signal of (4) and (6) are shown in Fig. 5 and Fig. 6, respectively.

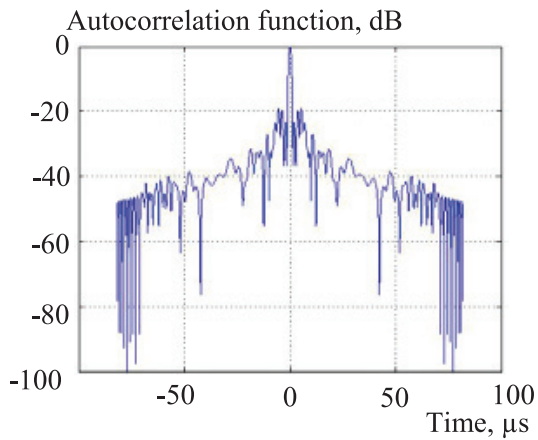
The parameters of the simulated signals are as follows: deviations of LFM fragments  $\Delta f_1 = \Delta f_3 = 125 \text{ kHz}$ ,  $\Delta f_2 = 300 \text{ kHz}$ , duration  $T_1 = T_3 = 20 \mu\text{s}$ ,  $T_2 = 100 \mu\text{s}$ , set that  $f_0 = \Delta f_1 + \Delta f_2 + \Delta f_3$ .



(a)



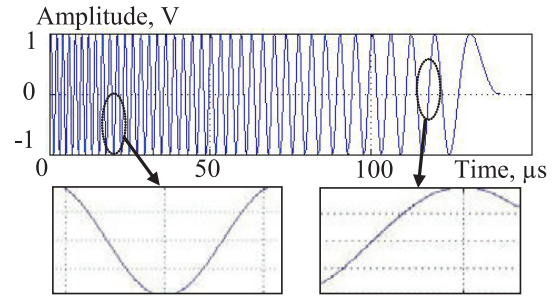
(b)



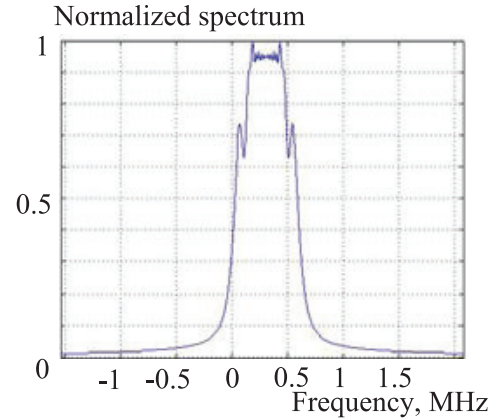
(c)

Fig. 5. Oscilloscope with detail at the joints of the fragments (a), spectrum (b), ACF (c) according to model (4)

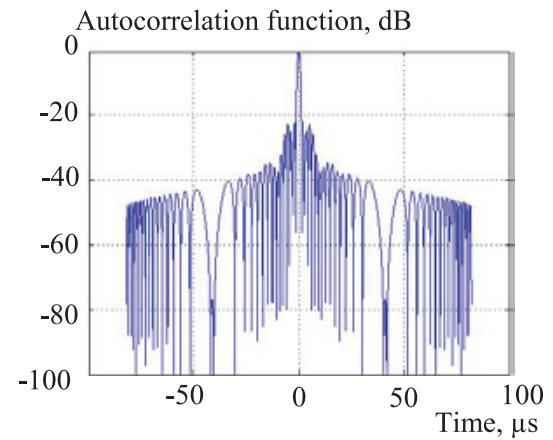
On the oscilloscope of the NLFM signal, Fig. 5a, there are phase jumps at the joints of the LFM fragments (timestamps of 20  $\mu\text{s}$  and 120  $\mu\text{s}$ ), which are shown on an enlarged scale for better clarity. These phase jumps cause distortion of the NLFM spectrum of the signal shown in Fig. 5b, that is, there are dips at the frequencies of transitions to the next fragment, the top of the spectrum is bevelled, there are pulsations on the side slopes.



(a)



(b)



(c)

Fig. 6. Oscilloscope with detail at the joints of the fragments (a), spectrum (b), ACF (c) according to model (6)

ACF signal, Fig. 5c, has MRBP -19.05 dB and ML width at a zero level of 4.92  $\mu\text{s}$ , ACF rays are distorted. In NLFM signal according to the improved model (6), phase jumps at the joints of NLFM signal fragments are compensated, as evidenced by the oscilloscope of Fig. 6a. Accordingly, the appearance of the signal spectrum of Fig. 6b changed for the better – it became symmetrical, without dips and pulsations on the slopes, the apex is flat. ACF, Fig. 6c, also demonstrates positive changes: MPSLL decreased to

-22.17 dB, ACF ML width is 4.85  $\mu$ s at zero level, the level of side lobes decreases and the frequency of their pulsations changes evenly. The decay rate of the ACF side lobes is 19.2 dB/deck.

Table 1 shows the results of comparison of LFM ACF and NLFM signal parameters with a total duration of 140  $\mu$ s and frequency deviation of 550 kHz.

Analysis of the data in Table 1 indicates a 65% decrease in MPSLL with a 31% expansion of the ACF ML for the three-fragment NLFM signal. It should be noted that the rate of decline in the level of the side lobes increased by 7%.

## Conclusions

Thus, the paper proposes improved MM with time shift for two- and three-fragment NLFM signals. The introduction of compensating phase components provides for a smooth change in the instantaneous phase of signals during the transition from the current FM fragment to the next. For the first time,

analytical expressions were obtained to calculate such components.

In comparison with the well-known models of NLFM signals, the use of improved MM provides for the case of a two-fragment NLFM signal a decrease in MPLSS by 1.4 dB with an almost equivalent width of ACF ML, and for a three-fragment NLFM signal a decrease in MPLSS is 3.12 dB with a slight (1.4%) narrowing of ACF ML.

The results of comparing the ACF of the three-fragment NLFM signal, which is more widely used in solving applied problems, and the classical LFM signal indicate that there is a decrease in MPSLL by 65% with the expansion of the ACF ML by 31%, while the rate of decline of the level of the ACF side lobes increases by 7%.

The introduction of advanced MM will contribute to the wider use of NLFM signals in various scientific and technical fields. Further research is planned to be directed at the features of using the developed mathematical models in solving applied problems in radar systems.

Table 1 Relative change of ACF signals parameters

Parameter name	LFM	NLFM	Percentage change, %
Width ML ACF, $\mu$ s	3,69	4,85	31
MPSLL, dB	-13,42	-22,17	65
decline of ML speed, dB/deck	17,9	19,2	7

## References

- [1] Skolnik M. I. (1990). *Radar Handbook*. McGraw-Hill Professional, Second edition, 1200 p.
- [2] Van Trees H. L. (2001). *Detection, Estimation, and Modulation Theory, Part III: Radar-Sonar Processing and Gaussian Signals in Noise*. John Wiley & Sons, Inc.
- [3] Barton D. K. (2004). *Radar System Analysis and Modeling*. Artech House Publishers, 535 p.
- [4] Cook, C. E. and Bernfeld M. (1993). *Radar Signals: An Introduction to Theory and Application*. Artech House, 552 p.
- [5] Melvin W. L., Scheer J. A. (2013). *Principles of modern radar, Vol. II: Advanced techniques*, Sci Tech Publishing.
- [6] Levanon N., and Mozeson E. (2004). *Radar Signals*. Wiley IEEE Press.
- [7] Hryzo A., Alchakov O., Lashkul I., Poltavec V. (2019). Suggestions on the Use of Multifrequency Signal for Upgrading of Jammer Protection Modernized P-18MA and P-18 Malakhit Radar. *Science and Technology of the Air Force of Ukraine*, No. 2(35), pp. 143-50. doi: 10.30748/nitps.2019.35.18.
- [8] Riabukha, V. P., Semeniaka, A. V., Katiushyn, Y. A., et al. (2022). Comparative Experimental Investigations of Adaptive and Non-adaptive MTI Systems in Pulse Radars of Various Applications and Wave Ranges. *Radioelectronics and Communications Systems*, Vol. 65, No. 4, pp. 165-176. doi: 10.3103/S073527272204001X.
- [9] Arnab Das, Venugopalan Pallayil. (2016). Analysis of Effective Signal Design for Active Sensing of Undersea Objects/Bottoms in Tropical Shallow Waters. *Conference OCEANS*. doi:10.1109/OCEANSAP.2016.7485558.
- [10] Song Chen, et al. (2022). A Novel Jamming Method against SAR Using Nonlinear Frequency Modulation Waveform with Very High Sidelobes. *Remote Sensing*, Vol. 14, Iss. 21, 5370. doi:10.3390/rs14215370.
- [11] Anoosha Chukka and Krishna B. T. (2022). Peak Side Lobe Reduction analysis of NLFM and Improved NLFM Radar signal. *AIUB Journal of Science and Engineering (AJSE)*, Vol. 21, Iss. 2, pp. 125–131. doi:10.53799/ajse.v21i2.440.
- [12] Adithyavalli N., Rani D. E., Kavitha C. (2019). An Algorithm for Computing Side Lobe Values of a Designed NLFM function. *International Journal of Advanced Trends in Computer Science and Engineering*, Vol. 8, No. 4, pp. 1026-103. doi:10.30534/ijatcse/2019/07842019.
- [13] Valli N. A., Rani D. E., Kavitha C. (2019). Modified Radar Signal Model using NLFM. *International Journal of Recent Technology and Engineering (IJRTE)*, Vol. 8, Iss. 2S3, pp. 513-516. doi: 10.35940/ijrte.B1091.0782S319.
- [14] Jeevanmai R., Rani N. D. (2016). Side lobe Reduction using Frequency Modulated Pulse Compression Techniques in Radar. *International Journal of Latest Trends in Engineering and Technology*, Vol. 7, Iss. 3, pp. 171-179. doi:10.21172/1.73.524.
- [15] Chan Y. K., Yam C. M., Koo V. C. (2009). Side lobes reduction using simple two and tri-stages non linear frequency modulation (NLFM). *Progress in Electromagnetics Research*, Vol. 98, pp. 33-52. doi:10.2528/PIER09073004.

- [16] Kostyria O. O., Hryzo A. A., Dodukh O. M. et al. (2023). Mathematical model of the current time for three-fragment radar signal with non-linear frequency modulation. *Radio Electronics, Computer Science, Control*, Vol. 3 (66). (In press).
- [17] Galushko V. G. (2019). Performance Analysis of Using Tapered Windows for Sidelobe Reduction in Chirp-Pulse Compression. *Radio Physics and Radio Astronomy*, Vol. 24, Iss. 4, pp. 300-313. doi:10.15407/rpra24.04.300.
- [18] Jeyanthi J. E., Shenbagavalli A., Mani V. R. S. (2017). Study of Different Radar Waveform Generation Techniques for Automatic Air Target Recognition. *International Journal of Engineering Technology Science and Research*, Vol. 4, Iss. 8, pp. 742-747.
- [19] Swiercz E., Janczak D., Konopko K. (2022). Estimation and Classification of NLFM Signals Based on the Time-Chirp Representation. *Sensors*, Vol. 22, Iss. 21, 8104. doi: 10.3390/s22218104.
- [20] Valli N. A., Rani D. E., Kavitha C. (2019). Windows for Reduction of ACF Sidelobes of Pseudo-NLFM Signal. *International Journal of Scientific & Technology Research*, Vol. 8, Iss. 10, pp. 2155-2161.
- [21] Ghavamirad R., Sebt M. A. (2019). Side lobe Level Reduction in ACF of NLFM Waveform. *IEE Radar, Sonar & Navigation*, Vol. 13, Iss. 1, pp. 74-80. doi:10.1049/iet-rsn.2018.5095.
- [22] Valli N. A., Rani D. E., Kavitha C. (2019). Doppler Effect Analysis of NLFM Signals. *International Journal of Scientific & Technology Research*, Vol. 8, Iss. 11, pp. 1817-1821.
- [23] Parwana S., Kumar S. (2015). Analysis of LFM and NLFM Radar Waveforms and their Performance Analysis. *International Research Journal of Engineering and Technology (IRJET)*, Vol. 02, Iss. 02, pp. 334-339.
- [24] Doerry A. W. (2006). Technical Report: SAR Processing with Non-Linear FM Chirp Waveforms. *Sandia National Laboratories*, 66 p. doi:10.2172/902597.
- [25] Alphonse S., Williamson G. A. (2014). Novel radar signal models using nonlinear frequency modulation. *22nd European Signal Processing Conference (EUSIPCO)*, pp. 1024-1028. doi:10.5281/ZENODO.44184.
- [26] Kavitha C., Valli N. A., Dasari M. (2020). Optimization of two-stage NLFM signal using Heuristic approach. *Indian Journal of Science and Technology*, Vol. 13, Iss. 44, pp. 4465-4473. doi:10.17485/IJST/v13i44.1841.
- [27] Kurdzo J. M., et al. (2014). A Pulse Compression Waveform for Improved-Sensitivity Weather Radar Observations. *Journal of Atmospheric and Oceanic Technology*, Vol. 31, Iss. 12, pp. 2713-2731. doi:10.1175/JTECH-D-13-00021.1.
- [28] Zhao Y., et al. (2020). Non-continuous piecewise nonlinear frequency modulation pulse with variable sub-pulse duration in a MIMO SAR Radar System. *Remote Sensing Letters*, Vol. 11, Iss. 3, pp. 283-292. doi:10.1080/2150704X.2019.1711237.
- [29] Alphonse S. and Williamson G. A. (2019). Evaluation of a class of NLFM radar signals. *EURASIP Journal on Advances in Signal Processing*, Article number: 62, 12 p. doi:10.1186/s13634-019-0658-9.
- [30] Gomi K., et al. (2017). Pulse Compression Weather Radar with Improved Sensitivity, Range Resolution, and Range Sidelobe. *38th Conference on Radar Meteorology*, Poster Session 131, pp. 1-7.
- [31] Jin G. et al. (2019). An Advanced Nonlinear Frequency Modulation Waveform for Radar Imaging With Low Sidelobe. *IEEE Transactions on Geosciences and Remote Sensing*, Vol. 57, pp. 6155-6168. DOI:10.1109/TGRS.2019.2904627.
- [32] Fan Z., Meng H. (2021). Coded excitation with Nonlinear Frequency Modulation Carrier in Ultrasound Imaging System. *2020 IEEE Far East NDT New Technology & Application Forum (FENDT)*, pp. 31-35. doi:10.1109/FENDT50467.2020.9337517.
- [33] Prakash B. L., Sajitha G. and Rajeswari K. R. (2016). Generation of Random NLFM Signals for Radars and Sonars and their Ambiguity Studies. *Indian Journal of Science and Technology*, Vol. 9, Iss. 29, pp. 1-7. doi:10.17485/ijst/2016/v9i29/93653.
- [34] Saleh M., Omar S.-M., Grivel E., Legrand P. (2021). A Variable Chirp Rate Stepped Frequency Linear Frequency Modulation Waveform Designed to Approximate Wideband Non-Linear Radar Waveforms. *Digital Signal Processing*, Vol. 109, 102884. doi:10.1016/j.dsp.2020.102884.
- [35] Xu Z., Wang X., Wang Y. (2022). Nonlinear Frequency-Modulated Waveforms Modeling and Optimization for Radar Applications. *Mathematics*, Vol. 10, Iss. 21, 3939. doi:10.3390/math10213939.

## Удосконалення математичних моделей зі зсувом часу дво- та трифрагментного сигналів з нелінійною частотною модуляцією

Костиря О. О., Гризо А. А., Додух О. М., Нарезній О. П.

Використання у радіолокаційних системах сигналів із внутрішньо-імпульсною модуляцією дозволяє збільшити тривалість зондувальних імпульсів, а значить і випромінювану енергію при обмеженнях на пікову потужність. Стиснення сигналу в системі обробки забезпечує необхідне розрізнення за часом, але призводить до появи бічних пелюсток. Це в свою чергу обумовлює «розтягування» зони пасивних перешкод за дальністю та погіршує потенційні можливості з виявлення цілей. Тому зниження рівня бічних пелюсток обробленого сигналу є актуальним завданням радіолокації. Стосовно максимального рівня бічних пелюсток переваги мають сигнали з нелінійною частотною модуляцією, але моделі, що використовуються для їх математичного опису, потребують уточнення. Проведені авторами статті дослідження та отримані результати математичного моделювання пояснюють механізм виникнення стрибків частоти та фази в сигналах з нелінійною частотною модуляцією, що складаються з кількох лінійно-частотно модульованих фрагментів. Зазначені результати отримано для математичної моделі поточного часу, тобто, коли час кожного наступного фрагменту відраховується від кінця попереднього. У статті розглядаються математичні моделі дво- та трифрагментних сигналів, які використовують інший підхід. Відмінність полягає, у тому, що початковий час кожного наступного лінійно-частотно модульованого фрагменту зсувається на початок відліку, тобто використовується зсунутий час. Перевагою цього підходу є відсутність стрибків частоти

на стиках фрагментів, але стрибки фази в ці моменти часу все рівно спостерігаються. Таким чином існує потреба у розробці математичного апарату компенсації таких стрибків. Аналіз відомих публікацій, проведений у першому розділі статті, показує, що для математичних моделей зсунутого часу питання визначення величини стрибків фази на стиках фрагментів та механізми їх компенсації не розглядалися. З цього витікає завдання дослідження, яке сформульовано у другому розділі роботи. Математичні викладки щодо визначення величини фазових стрибків, які виникають в зазначених

математичних моделях, а також результати перевірки удосконаленого математичного апарату наведено у третьому розділі роботи. Подальші дослідження плануються спрямувати на особливості використання розроблених математичних моделей при вирішенні прикладних завдань у радіолокаційних системах.

*Ключові слова:* сигнали з нелінійною частотною модуляцією; математична модель; стрибок миттєвої фази; автокореляційна функція; максимальний рівень бічних пелюсток